Neurobiology of Aging 51 (2017) 97–103

Contents lists available at ScienceDirect

Neurobiology of Aging

journal homepage: www.elsevier.com/locate/neuaging

White matter lesions relate to tract-specific reductions in functional connectivity

Carolyn D. Langen [a,b], Hazel I. Zonneveld [a,c], Tonya White [a,d], Wyke Huizinga [a,b], Lotte G.M. Cremers [a,c], Marius de Groot [a,b,c], Mohammad Arfan Ikram [a,c], Wiro J. Niessen [a,b,e], Meike W. Vernooij [a,c,*]

[a] Department of Radiology and Nuclear Medicine, Erasmus MC - University Medical Center Rotterdam, Rotterdam, the Netherlands
[b] Department of Medical Informatics, Erasmus MC - University Medical Center Rotterdam, Rotterdam, the Netherlands
[c] Department of Epidemiology, Erasmus MC - University Medical Center Rotterdam, Rotterdam, the Netherlands
[d] Department of Child and Adolescent Psychiatry, Erasmus MC - University Medical Center Rotterdam, Rotterdam, the Netherlands
[e] Department of Imaging Physics, Faculty of Applied Sciences, Delft University of Technology, Delft, the Netherlands

ARTICLE INFO

Article history:
Received 4 August 2016
Received in revised form 19 October 2016
Accepted 5 December 2016
Available online 14 December 2016

Keywords:
Lesions
Function
Brain
Location-specific
Connectivity

ABSTRACT

White matter lesions play a role in cognitive decline and dementia. One presumed pathway is through disconnection of functional networks. Little is known about location-specific effects of lesions on functional connectivity. This study examined location-specific effects within anatomically-defined white matter tracts in 1584 participants of the Rotterdam Study, aged 50–95. Tracts were delineated from diffusion magnetic resonance images using probabilistic tractography. Lesions were segmented on fluid-attenuated inversion recovery images. Functional connectivity was defined across each tract on resting-state functional magnetic resonance images by using gray matter parcellations corresponding to the tract ends and calculating the correlation of the mean functional activity between the gray matter regions. A significant relationship between both local and brain-wide lesion load and tract-specific functional connectivity was found in several tracts using linear regressions, also after Bonferroni correction. Indirect connectivity analyses revealed that tract-specific functional connectivity is affected by lesions in several tracts simultaneously. These results suggest that local white matter lesions can decrease tract-specific functional connectivity, both in direct and indirect connections.

1. Introduction

The importance of healthy white matter for brain functioning is becoming increasingly understood. White matter atrophy and white matter lesions (WMLs), both markers of white matter pathology which can be assessed using imaging, have been related to cognitive decline (Debette and Markus, 2010; Griebe et al., 2014), impairment in gait (Starr et al., 2003), depression (Dalby et al., 2012), and an increased risk of stroke and dementia (Debette and Markus, 2010). White matter is organized in the brain in tracts, which connect functional brain regions with each other or project outside the brain, mostly to the spinal cord. When the integrity of these white matter tracts is compromised, one might expect that a deficit in function will follow; this has been coined the "disconnection hypothesis" (Friston, 1998). In this hypothesis, a loss of connections in brain structure (i.e., white matter connections) directly affects brain functioning, or so-called functional connectivity (i.e., gray matter activity).

Experimental evidence from animal studies indeed suggests that functional connectivity is negatively affected by white matter disconnection (O'Reilly et al., 2013; van Meer et al., 2010). Evidence supporting the disconnection hypothesis in humans has been found in individual patients with tumors (Schonberg et al., 2006), after stroke (Seghier et al., 2004; Song et al., 2014), after transection of the corpus callosum (Johnston et al., 2008), and damage to the arcuate fasciculus resulting in nonfluent speech production in aphasia (Fridriksson et al., 2013). These studies, however, focused only on neurological events and conditions affecting single individuals with rare events. This relationship has not yet been confirmed on a population level for more common, yet arguably more subtle pathologies, such as WMLs. In the general population, white matter pathology has indeed been linked to reductions in neuronal activity on a global level (Griebe et al., 2014; Zhou et al., 2015), but it is still poorly understood how pathology affects functional connectivity on a local level, that is, specific tracts and

* Corresponding author at: Department of Epidemiology, Erasmus MC - University Medical Center Rotterdam, P.O. Box 2040, 3000 CA Rotterdam, the Netherlands. Tel.: +31 10 70 42006; fax: +31 10 70 44657.
E-mail address: m.vernooij@erasmusmc.nl (M.W. Vernooij).

0197-4580/$ – see front matter © 2016 Elsevier Inc. All rights reserved.
http://dx.doi.org/10.1016/j.neurobiolaging.2016.12.004

their connecting brain regions. It is important that we gain more insight into this relation, as it may help us to understand why there is a large inter-individual variation in how white matter pathology compromises brain function. Also, it could help us predict in which brain regions white matter pathology will cause more functional deficits, which may ultimately enable prevention and earlier therapy. With this in mind, we examined the location-specific relationship between WMLs and functional connectivity within a population-based setting of middle-aged and older adults.

2. Material and methods

2.1. Setting

The study was embedded within the Rotterdam Study, a large population-based cohort designed to investigate chronic diseases in middle-aged and older population (Hofman et al., 2015). The cohort originated in 1990 and comprised 7983 participants aged 55 years and older. In 2000 and 2006 the cohort was expanded and now includes 14,926 participants aged 45 years and older. Brain magnetic resonance imaging (MRI) was implemented in the core study protocol from 2005 onwards. The Rotterdam Study has been approved by the medical ethics committee according to the Population Study Act Rotterdam Study, executed by the Ministry of Health, Welfare and Sports of the Netherlands. Written informed consent was obtained from all participants.

Resting-state functional MRI (rs-fMRI) was piloted in 2009–2011, and implemented into the existing multi-sequence study protocol from 2012 onwards. Between January 2009 and October 2013 we obtained rs-fMRI from 2118 participants. We excluded participants with prevalent dementia at time of scanning (n = 5), insufficient screening for dementia (n = 12), relative motion (i.e., the amount of movement between 2 consecutive time points) of >0.5 mm (n = 1) or absolute motion >3 mm in any volume in the rs-fMRI (n = 46), or image artifacts interfering with data extraction on any of the scans necessary for this study (e.g., due to metal artifacts, registration issues) (n = 158). Furthermore, we excluded scans with cortical infarcts (n = 65), because gliosis around cortical infarcts may cause automated WML segmentation to become unreliable. In total, 1831 rs-fMRI scans were available for analysis. Of these, n = 71 were excluded because of missing diffusion data, n = 159 were excluded because of partially scanned occipital or temporal lobes in the rs-fMRI and n = 17 were excluded because of failed cortical parcellation, yielding a total of n = 1584 for the current analysis.

2.2. Image acquisition

Participants were scanned on a 1.5 tesla GE Signa Excite scanner. This included a T1-weighted image (T1w, repetition time [TR] = 13.8 ms, echo time [TE] = 2.80 ms, inversion time [TI] = 400 ms, 96 slices of 1.6 mm), a T2-weighted fluid-attenuated inversion recovery sequence (TR = 8000 ms, TE = 120 ms, TI = 2000 ms, 64 slices of 2.5 mm), a proton density weighted image (TR = 21,300 ms, TE = 17.3, 90 slices of 1.6 mm), a spin echo echo-planar diffusion-weighted image (DWI, TR = 8000 ms, TE = 74.6 ms, axial field of view 210 × 210 mm, 39 contiguous slices of 3.5 mm, maximum b-value 1000 mm^2/s in 25 noncollinear directions with 3 unweighted volumes), and an rs-fMRI sequence (TR = 2900 ms, TE = 60 ms, 31 slices of 3.3 mm, 160 time points 2.9 seconds apart). Additional details about the image acquisition can be found in (Ikram et al., 2015).

2.3. Image processing

Tissue segmentation, DWI processing and white matter tract segmentation procedures were similar to those described in (de Groot et al., 2015). Briefly, structural MRIs were automatically segmented into gray matter, white matter and CSF using a k-nearest-neighbors classifier (Vrooman et al., 2007). Tissue segmentations and fluid-attenuated inversion recovery intensity were used to segment WMLs using an automated approach (de Boer et al., 2009). Lesion segmentations were manually inspected, and corrected in the case of errors. WML segmentations were affinely transformed to diffusion space. DWI volumes were coregistered to reduce the effect of participant motion and eddy currents. The resulting rotation parameters were used to correct gradient vectors. A diffusion model was estimated from the coregistered DWI, and probabilistic tractography was used to reconstruct white matter fibers using BEDPOSTX and PROBTRACKX (Behrens et al., 2003, 2007), respectively, both of which are available in the FMRIB software library (FSL, http://www.fmrib.ox.ac.uk/fsl/) (Jenkinson et al., 2012). AutoPtx was used to identify white matter tracts (de Groot et al., 2015). For each tract this produced a tract-density image, which was then normalized and thresholded using tract-specific thresholds that were previously extensively optimized based on the reproducibility of fractional anisotropy measurements in 30 subjects of the Rotterdam Study (de Groot et al., 2015). Of the 26 reconstructed tracts, this study included 2 interhemispheric tracts (forceps major and minor) and 18 intrahemispheric tracts (9 pairs of tracts with 1 tract per hemisphere). The remaining tracts were excluded because they projected into tissues outside of the brain. AutoPtx tracks the cingulum in 2 parts (i.e., the cingulate-gyral and parahippocampal parts). In each hemisphere, the 2 parts were combined to form a single tract. Each intrahemispheric tract had a left and right component, thus a total of 18 tracts were included in these analyses. A list of included tracts and their anatomical descriptions can be found in Supplementary Table 1. Tract-specific measurements of WML volume and white matter volume were computed after thresholding tract images as described in (de Groot et al., 2015).

The rs-fMRI data was preprocessed using FSL. This included affine registration with 12 degrees of freedom of rs-fMRI volumes to the individual's T1w structural image using FMRIB's linear image registration tool, and a nonlinear registration of the T1w image to a standard space template (MNI 152) using FMRIB's non-linear image registration tool (Andersson et al., 2007). All registrations were visually inspected and excluded if they were of poor quality. Low-frequency drifts and motion components were compensated for using MCFLIRT and temporal filtering (Beckmann and Smith, 2004; Jenkinson et al., 2002). The resulting image was decomposed into several components using single-session independent component analysis. In a test set of 60 participants that were equally distributed over 5 age groups (aged 50–59.4 year, 59.4–68.4 year, 68.5–77.3 year, 77.3–86.3 year, 86.7+ year) and gender, the components were manually (visually) classified as "good" (signal) or "bad" (noise) components. This was used to denoise the rs-fMRI data using FMRIB's ICA-based Xnoiseifier 1.06 (FIX) (Griffanti et al., 2014; Salimi-Khorshidi et al., 2014).

In order to compute tract-specific functional connectivity, masks of the gray matter voxels corresponding to either end of each tract were defined. To this end, T1w images were first parcellated by FreeSurfer into cortical (34 parcels per hemisphere) and subcortical parcellations (Fischl, 2012). FreeSurfer cortical parcels were further subdivided into 241 regions of interest (ROIs) using the Connectome Mapper's python nipype interface (Daducci et al., 2012; Gorgolewski et al., 2011). This parcellation resolution was chosen because the regions were relatively small, yet allowed better

correspondence across participants than higher resolutions (Cammoun et al., 2012). When delineating cortical ROIs, the connectome mapper labels only the voxels on the border between the white matter and cortex. The remaining cortical voxels were assigned the ROI labels of the closest labeled voxel. The entire ROI volume was affinely transformed to diffusion space. For a given unthresholded tract, ROIs that did not overlap with the unthresholded tract image in at least 90% of participants were excluded. A threshold was not used in order to ensure that projections into the gray matter, which are less dense than in the middle of the tract, are left intact. ROIs were further excluded if they did not conform to commonly accepted definitions of the endpoints of the tract (see Supplementary Table 1) (Wakana et al., 2004), were found in the middle portion of a tract, or if it was ambiguous to which end of the tract the ROI belonged. For example, the uncinate fasciculus connects frontal and temporal regions, where the insula is positioned in the middle portion of the tract. In this case, it is unclear whether the insula belongs to the frontal or temporal end of the tract, and the degree of connectivity with the insula is unknown. For this reason, the insula was deemed a region that would confound the results and thus was not included in the analysis of the uncinate fasciculus. Each included ROI was assigned to either end of the tract. See Supplementary Table 1 for a list of ROIs corresponding to each tract.

Functional connectivity was computed for each tract. To do this, the ROI segmentation and each white matter tract were transformed into fMRI space. Two masks per tract were formed by taking the intersection of the unthresholded tract and the identified ROIs. A mean time-series was computed across all voxels within each mask from the preprocessed fMRI data. Functional connectivity for a given tract was calculated as the Pearson correlation of the mean time-series within the 2 masks corresponding to the tract.

2.4. Statistical analysis

The relationship between age and both tract-specific WML volume and functional connectivity was determined using Spearman's correlation. Robust linear regression models were fit per tract to determine how both global (i.e., brain-wide, model 1) and local (i.e., tract-specific, model 2) WMLs affect functional connectivity across each tract using the statsmodels Python library (http://statsmodels.sourceforge.net). We used robust linear regression because it minimizes the effect of outliers on the model fitting. Model 2 additionally included the tract's white matter volume as a covariate. Model 2 measured the associations in direct connections (i.e., both functional connectivity and WML volume were from the same tract). A third model was fit to all possible pairs of tracts to determine how WMLs in indirect connections affect functional connectivity. In this model, the functional connectivity in a given tract was the dependent variable, the WML volume of a second tract was the independent variable of interest, where the white matter volume of the second tract was included as a covariate. All 3 models included intracranial volume, age, and gender as covariates. All variables and covariates except for gender were standardized before model fitting. Given that the models had multiple outcome measures and input variables (M = 18 for both functional connectivity and tract-specific WML load), there were 2 sources of dependence between tests. Thus, standard methods of adjusting for multiple testing in the case of dependent variables, which only consider the case of multiple outcome measures with a single global dependent variable of interest, were not applicable. In order to take type I errors into account, we considered significance over a range of p-values between 0.05 and the Bonferroni threshold 0.05/M = 0.0028 and evaluated significant results in each tract relative to each other.

Table 1
Characteristics of the study population

Characteristics	N = 1584
Age, y	62.6 (6.5, range: 50–95)
Female	929 (58.6)
Global white matter lesion volume, mL	4.0 (1.5–4.3)
Global normal-appearing white matter volume, mL	409.6 (54.6)
Intracranial volume, mL	1133.1 (111.0)

Data presented as mean (standard deviation) for continuous variables and number (percentages) for categorical variables. White matter lesion volume presented as median (interquartile range).

3. Results

The characteristics of the study population are shown in Table 1. Of the 1584 participants, the mean age was 62.6 years (standard deviation 6.5, age range 50–95 years), and 58.6% were women. The median WML volume was 4.0 mL (interquartile range 1.5–4.3). WMLs were concentrated primarily within the forceps major, anterior thalamic radiations, posterior thalamic radiations and inferior longitudinal fasciculi, however WML load (i.e., WML volume adjusted for tract volume), was found in all tracts (see Fig. 1A). T-tests indicated that the mean WML load for all tracts was significantly different from zero, with the largest p-value being less than 10^{-18}. Tract-specific functional connectivity varied greatly across tracts and participants (see Fig. 1B), where the greatest sample means were found in forceps major and minor and smallest sample means were found in the uncinate fasciculi and posterior thalamic radiations. WML volume was highly positively correlated ($p < 0.0028$) with age in all tracts, whereas functional connectivity was highly negatively correlated ($p < 0.0028$) with age in the uncinate fasciculi, cingulate gyri, and forceps minor (Fig. 2). Gray matter ROIs included for each tract are visualized in Supplementary Fig. 1.

The relationship between WML load and functional connectivity varied greatly across tracts and between hemispheres. Figs. 3 and 4 show how functional connectivity decreased with increasing WML volume. The association between higher tract-specific WML load and lower functional connectivity in direct connections reached Bonferroni significance ($p < 0.0028$) in the left inferior fronto-occipital fasciculus whereas the relationship between global WML volume and functional connectivity did not reach Bonferroni significance in any tract (Fig. 3). The global and local associations in several tracts approached statistical significance ($0.0028 < p < 0.05$), all of which indicated that increased WML volume is associated with decreased functional connectivity. Of the associations with $p < 0.05$, age played a highly significant role ($p < 0.0028$) only in the global model for the uncinate fasciculi and the right cingulate gyrus.

The functional connectivity of most tracts decreased with increasing WML volume in several other tracts, which is summarized in Fig. 5 (model 3, see Supplementary Fig. 2 for a visualization of the results in connectivity diagrams). In other words, the functional connectivity across a given tract is often negatively affected by WMLs in indirect connections. The functional connectivity across most association tracts were often affected by WML load in association, limbic and projection tracts, where the Bonferroni threshold ($p < 0.0028$) was reached in 4 tracts. Of the projection tracts, the functional connectivity across only the left anterior and right superior thalamic radiation was affected by the WML volume in several tracts. The functional connectivity of the forceps major was affected by the WML volume in association and projection tracts with significance that approached the

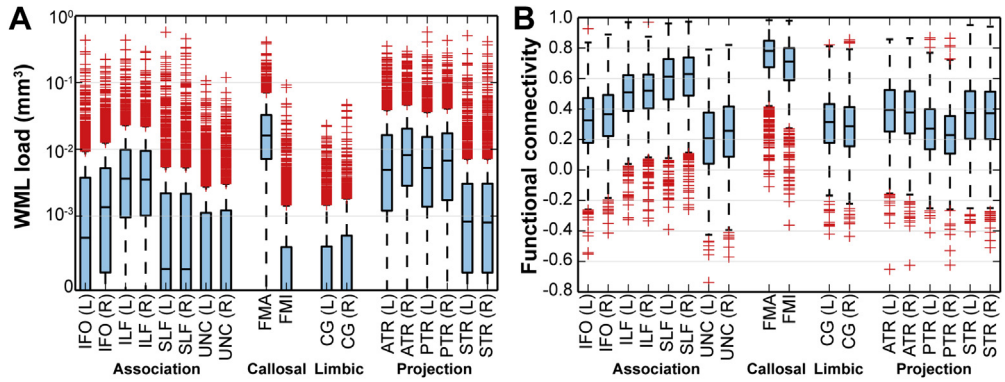

Fig. 1. Distribution of tract-specific white matter lesion (WML) load and functional connectivity across participants. Boxes extend from the lower to the upper quartile, where the median is indicated by a line. Whiskers indicate the range of values within 1.5 times the interquartile range from the median. Red markers show individual observations outside of the whisker range. White matter tracts are listed alphabetically on the x-axis. In (A) WML load is on the y-axis and is defined as the volume of WMLs in a given tract divided by tract volume. In (B) functional connectivity is on the y-axis and is defined as the Pearson correlation of the mean time-series within the regions on either end of a given tract. Abbreviations: ATR, anterior thalamic radiations; CG, cingulum bundle; FMA, forceps major; FMI, forceps minor; IFO, inferior fronto-occipital fasciculus; ILF, inferior longitudinal fasciculus; PTR, posterior thalamic radiations; SLF, superior longitudinal fasciculus; STR, superior thalamic radiations; UNC, uncinate fasciculus; and (L) and (R) indicate that a tract is in the left or right hemisphere, respectively. (For interpretation of the references to color in this figure legend, the reader is referred to the Web version of this article.)

Bonferroni threshold ($0.0028 < p < 0.05$), whereas the functional connectivity in limbic tracts and the forceps minor were largely unaffected by WMLs. Bonferroni significance was reached for 9 associations, 3 of which affected the functional connectivity in the right anterior thalamic radiation, 2 of which affected the functional connectivity in the superior thalamic radiation and 4 of which affected the functional connectivity in association tracts Fig. 5. The WML volume in the left inferior fronto-occipital fasciculus, right superior longitudinal fasciculus (SLF) and posterior thalamic radiation each affected functional connectivity in 2 tracts with Bonferroni significance. Other tracts with Bonferroni level WML effects included the bilateral cingula and left SLF. Of the tracts with Bonferroni significance in relation to WML volume, functional connectivity was negatively associated with age in the uncinate fasciculi ($p < 0.0023$), the right anterior thalamic radiation ($p < 0.05$) and the right superior thalamic radiation ($p < 0.05$).

4. Discussion

In this large study among community-dwelling participants aged over 50 years, we found that a higher tract-specific WML load related to lower functional connectivity in the brain regions connecting to these tracts. This finding supports the "disconnection hypothesis" and is indicative of local structural pathology directly affecting brain function. Yet, we furthermore found that tract-specific functional connectivity was also influenced by white matter load in other, not directly connected tracts. This implies that also diffuse white matter pathology, or indirect connections, may affect functional connectivity.

This study benefited from a large sample size and the fact that both DWI and rs-fMRI were acquired in the same scanning session and with consistent scanning parameters. We also used advanced probabilistic tractography and tract segmentation methods which help to spatially localize anatomical tracts in native space.

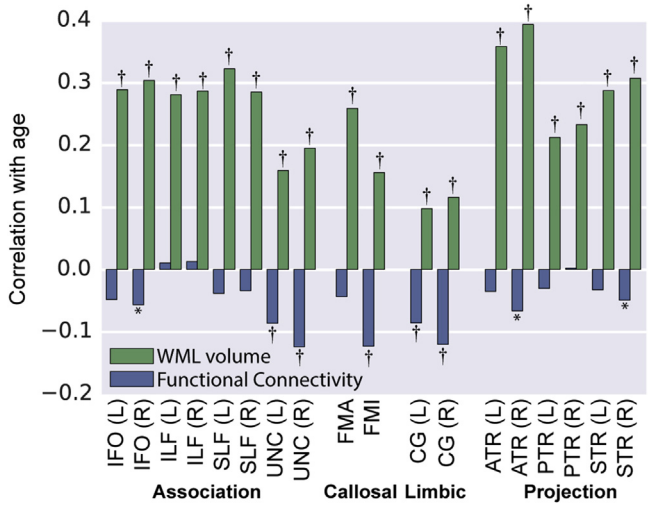

Fig. 2. Correlation of functional connectivity (blue) and white matter lesion (WML) volume (green) with age. †Indicates Bonferroni significance (i.e., $p < 0.0028$). *Indicates $p < 0.05$. (For interpretation of the references to color in this figure legend, the reader is referred to the Web version of this article.)

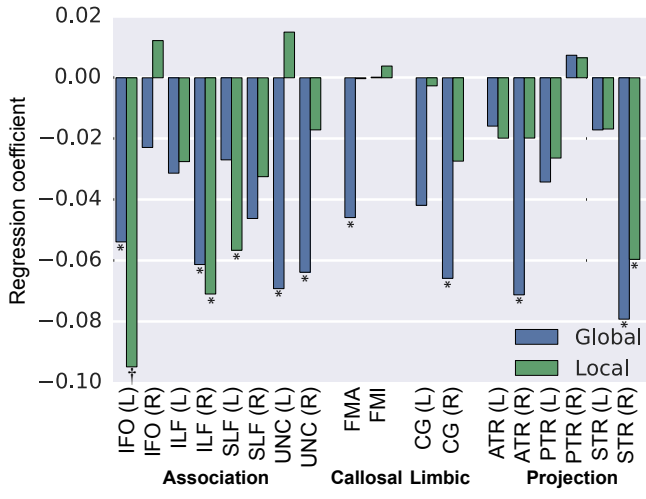

Fig. 3. Model parameters in direct connections. Blue and green bars show the parameters associated with global white matter lesion (WML) volume (WML_{global}) in model 1 and local WML volume (WML_{local}) in model 2, respectively. †Indicates Bonferroni significance (i.e., $p < 0.0028$). *Indicates $p < 0.05$. (For interpretation of the references to color in this figure legend, the reader is referred to the Web version of this article.)

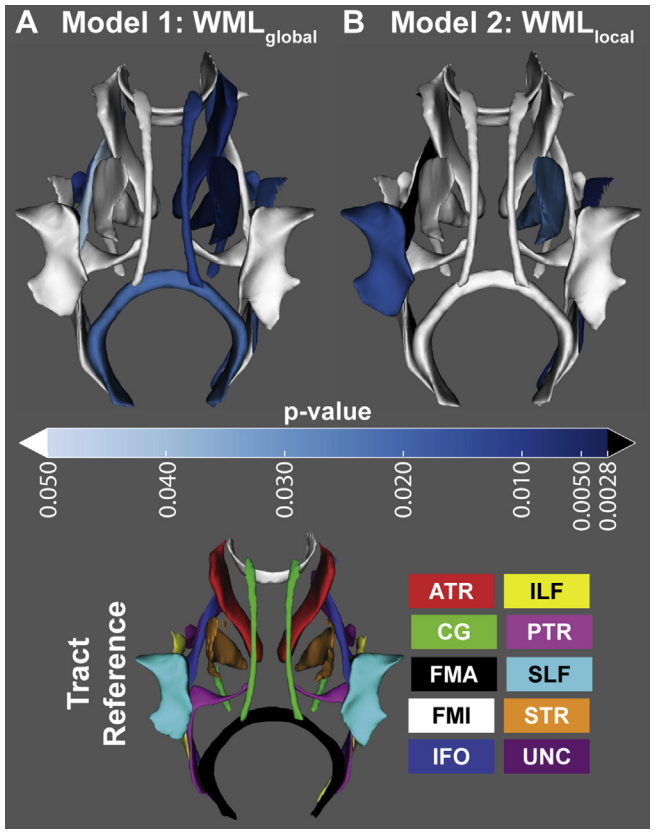

Fig. 4. The association between WML volume and functional connectivity in each tract. The *p*-values of the regression coefficient corresponding to (A) global WML volume (WML_{global}) in model 1 and (B) local WML volume (WML_{local}) in model 2 are represented by the color in each tract. Tracts that reached Bonferroni significance (i.e., $p < 0.0028$) are colored black. Shades of blue denote significant connections that did not reach Bonferroni significance. White denotes nonsignificance. The tract reference specifies the names associated with each tract. Abbreviations: ATR, anterior thalamic radiations; CG, cingulum bundle; FMA, forceps major; FMI, forceps minor; IFO, inferior fronto-occipital fasciculus; ILF, inferior longitudinal fasciculus; PTR, posterior thalamic radiations; SLF, superior longitudinal fasciculus; STR, superior thalamic radiations; UNC, uncinate fasciculus; WML, white matter lesion. (For interpretation of the references to color in this figure legend, the reader is referred to the Web version of this article.)

Additionally, we specifically concentrated on data, such as what is typically acquired in a standard clinical setting, where angular and spatial resolution is often limited, rather than advanced imaging protocols, to show that such methods are within the grasp of typical epidemiological and clinical studies. The study was limited by a cross-sectional design, in which it is not possible to ascertain whether WMLs cause a decrease in functional connectivity or vice versa, though the latter is biologically less likely. Also, our findings are supported by previous research that shows a reduction of functional connectivity following transection of the corpus callosum in a single participant, where the anterior and posterior commissures were left intact (Johnston et al., 2008). The analyses in this study were further limited by the fact that some tracts had a very low WML volume across participants. Although all tracts had a range of WML loads and for all tracts this load was significantly greater than zero, for some tracts WMLs were present only in a few subjects, and they were often small. For these tracts a decrease in functional connectivity may not yet be detectable. As such, we may have underestimated the impact of some strategic WMLs on functional connectivity. Additionally, a potential limitation is our choice to use anatomically-defined white matter tracts, which is on a relatively large scale and does not take all gray matter regions into account. A broader explorative approach such as connectomics would be more inclusive and less aggregated, but would require more rigorous multiple-testing correction, and result in more uncertainty about whether observed structural connections are representative of true anatomical connectivity, and a more difficult interpretation of results in a biological or psychological context. Another limitation related to the chosen method of delineating gray matter tract endpoint masks is the fact that the method assumes that white matter tracts are comprised predominantly of bundled axons projecting from one single location to another. In reality, some fibers join and leave these bundles at various points along the tract, which could not be modeled with the approach we used.

We found that global and local WML volume had a significant relationship with functional connectivity in many of the same tracts, which reflects both the contribution of each tract to the global white matter volume and the fact that functional connectivity is believed to be an amalgamation of both direct and indirect connections. Neuronal signals can travel from one region to another via intermediate regions and thus contribute to functional connectivity; hence the WML load of one tract may influence the functional connectivity across another. Indeed, our analyses found that the functional connectivity across a given tract was also influenced by the WML load in several other tracts, and that these indirect connections were often stronger than the direct associations. We were unable to include global WML load into the direct and indirect models because of multicollinearity issues. Because of this, we cannot conclusively claim that our results cannot be explained by systemic white matter disease burden. However, our analysis included the tracts which contain the majority of lesions, which together encompass most white matter that contributes to global WML load. Thus, these results estimate the relative contribution of WMLs in each tract, where the strongest relationships are likely driving forces in the loss of functional connectivity. This is supported by findings from animal studies. A study on rats found that after induced stroke, functional connectivity initially dropped but then was gradually restored, likely through indirect connections (van Meer et al., 2010). Another study on monkeys found that interhemispheric functional connectivity was partially maintained after complete section of the corpus callosum when another tract, the anterior commissure, was spared (O'Reilly et al., 2013). In humans, patients with either complete transection or absence of the corpus callosum had at least partially intact interhemispheric connectivity (Risse et al., 1978; Tyszka et al., 2011; Uddin et al., 2008), which might also arise from alternate pathways such as the anterior or posterior commissures. Thus, the brain's structural network allows brain function to be maintained via alternate pathways, even when direct connectivity is compromised. For example, the functional connectivity in the right anterior thalamic radiation (ATR) was affected by WMLs in 4 tracts, where the left inferior fronto-occipital fasciulus (IFO) and the bilateral SLF were all significant according to the Bonferroni threshold. The ATR, IFO and SLF all serve frontal regions. It is interesting that the functional connectivity of the bilateral IFO was not affected by the WML load in either the left or right ATR, suggesting that while the IFO may be an important alternate pathway for the ATR, the opposite may not be the case.

When interpreting these results, it has to be considered that age is correlated with functional connectivity and WML volume in several tracts. Given that age was included as a covariate in all models, it is remarkable that we still found several strong associations between WML volume and functional connectivity. This suggests that there is an age-independent and location-specific relation between WML volume and functional connectivity.

The results of this study have important implications with respect to cognition. Previous studies on a similar sample found that reduced global white matter integrity (estimated by diffusion

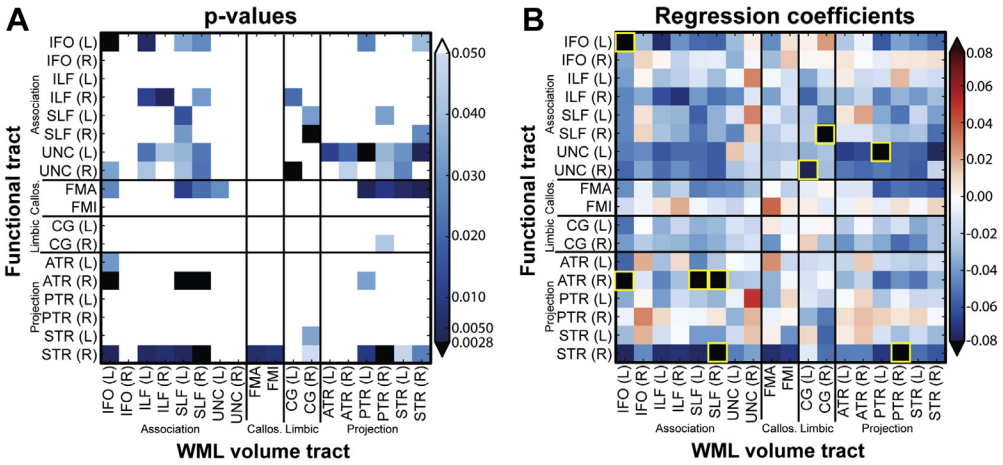

Fig. 5. The effect of WMLs in indirect connections on functional connectivity. Each matrix element corresponds to a single regression of model 3, where the WML volume of the tract on the x-axis is the independent variable and the functional connectivity across the tract on the y-axis is the dependent variable. The color of each element represents (A) the *p*-value and (B) the regression coefficient. In (A), tracts that reached Bonferroni significance (i.e., $p < 0.0028$) are colored black, shades of blue denote significant connections ($p < 0.05$) that did not reach Bonferroni significance, and white denotes nonsignificance. In (B), negative associations are in shades of blue, positive associations are in shades of red and significant associations ($p < 0.0028$) are outlined in yellow. All significant associations were negative. All models included tract-specific white matter volume, age, sex, and intracranial volume as covariates. Abbreviations: ATR, anterior thalamic radiations; CG, cingulum bundle; FMA, forceps major; FMI, forceps minor; IFO, inferior fronto-occipital fasciculus; ILF, inferior longitudinal fasciculus; PTR, posterior thalamic radiations; SLF, superior longitudinal fasciculus; STR, superior thalamic radiations; UNC, uncinate fasciculus; WML, white matter lesion; and (L) and (R) indicate that a tract is in the left or right hemisphere, respectively. (For interpretation of the references to color in this figure legend, the reader is referred to the Web version of this article.)

measures) related to worse cognitive function (Vernooij et al., 2009) as well as a tract-specific link between decline in white matter integrity and decline in cognitive function, independent of tract-specific WML volume, especially in the inferior fronto-occipital fasciculus (Cremers et al., 2016). We found that the left fronto-occipital fasciculus had a significantly worse tract-specific functional connectivity with higher local WML load. WMLs in this tract also had a significant relationship on the functional connectivity of several other tracts. Taking into account that WMLs and white matter microstructure are assumed part of the same disease spectrum (de Groot et al., 2013; Maillard et al., 2013), our study adds important insights to these previous findings in that it shows a local decline in brain function in relation to local white matter pathology. This provides a potential mechanism to explain the observed cognitive decline. While this study focused on WMLs, which are easily detected in structural images, future studies including microstructural parameters, such as fractional anisotropy and mean diffusivity, might shed additional light on the location-specific relationship between white matter degeneration and functional connectivity. Such a study would, however, be limited by the fact that deviations in the value of these parameters does not necessarily indicate pathology. Also, a simple average of values across an entire tract may not adequately represent the microstructural changes that precede lesion formation.

White matter disease is highly prevalent in aging, both in terms of macrostructural changes (atrophy and lesions) as well as microstructural abnormalities, and is considered to be mainly of vascular origin (Farrall and Wardlaw, 2009; Pantoni, 2010). Given that cerebral small vessel damage and WML development are increased by hypertension, a potential treatment to prevent WMLs from developing is to control blood pressure (Pantoni, 2010; Verhaaren et al., 2013). Future studies on whether WMLs can be prevented or even treated would add important insights into whether we can prevent or reduce loss of functional connectivity. Another important focus of future studies would be to determine why some tracts are more vulnerable to WML-related connectivity loss than others and to consider the importance of indirect connections on functional connectivity in relation to vascular disease.

In conclusion, we found that a higher tract-specific WML load relates to lower functional connectivity in the brain regions connecting to these tracts. This finding supports the “disconnection hypothesis” and is indicative of local structural pathology directly implicating brain function. The results of this study provide clues into the mechanism of reduced brain functioning as a result of WMLs on a local level.

Disclosure statement

The authors have no actual or potential conflicts of interest.

Acknowledgements

The authors would like to sincerely thank all those involved in the data collection and processing of the Rotterdam Study data. Henri Vrooman provided a great deal of assistance in assembling the required datasets and Martijn van den Heuvel provided valuable feedback in the concept development stage. This work was supported by the Netherlands Organisation for Health Research and Development (grant numbers 91211021, 90700435); the Netherlands Organisation for Scientific Research (grant 184.033.111); Alzheimer Nederland (grant WE.03-2012-30), the European Union Seventh Framework Programme (FP7/2007–2013) (grant FP7-ICT-2011-9-601055); the Erasmus MC and Erasmus University Rotterdam; the Research Institute for Diseases in the Elderly (RIDE); the Ministry of Education, Culture and Science; the Ministry of Health, Welfare and Sports; the gs7:European Commission; and the Municipality of Rotterdam.

Appendix A. Supplementary data

Supplementary data associated with this article can be found, in the online version, at http://dx.doi.org/10.1016/j.neurobiolaging.2016.12.004.

References

Andersson, J.L.R., Jenkinson, M., Smith, S., 2007. Non-linear Registration, Aka Spatial Normalisation FMRIB Technical Report TR07JA2. FMRIB Anal. Gr. Univ, Oxford.

Beckmann, C.F., Smith, S.M., 2004. Probabilistic independent component analysis for functional magnetic resonance imaging. IEEE Trans. Med. Imaging 23, 137–152.

Behrens, T.E.J., Berg, H.J., Jbabdi, S., Rushworth, M.F.S., Woolrich, M.W., 2007. Probabilistic diffusion tractography with multiple fibre orientations: what can we gain? Neuroimage 34, 144–155.

Behrens, T.E.J., Woolrich, M.W., Jenkinson, M., Johansen-Berg, H., Nunes, R.G., Clare, S., Matthews, P.M., Brady, J.M., Smith, S.M., 2003. Characterization and propagation of uncertainty in diffusion-weighted MR imaging. Magn. Reson. Med. 50, 1077–1088.

Cammoun, L., Gigandet, X., Meskaldji, D., Thiran, J.P., Sporns, O., Do, K.Q., Maeder, P., Meuli, R., Hagmann, P., 2012. Mapping the human connectome at multiple scales with diffusion spectrum MRI. J. Neurosci. Methods 203, 386–397.

Cremers, L.G.M., de Groot, M., Hofman, A., Krestin, G.P., van der Lugt, A., Niessen, W.J., Vernooij, M.W., Ikram, M.A., 2016. Altered tract-specific white matter microstructure is related to poorer cognitive performance: The Rotterdam Study. Neurobiol. Aging 39, 108–117.

Daducci, A., Gerhard, S., Griffa, A., Lemkaddem, A., Cammoun, L., Gigandet, X., Meuli, R., Hagmann, P., Thiran, J.-P., 2012. The connectome mapper: an open-source processing pipeline to map connectomes with MRI. PLoS One 7, e48121.

Dalby, R.B., Frandsen, J., Chakravarty, M.M., Ahdidan, J., Sørensen, L., Rosenberg, R., Østergaard, L., Videbech, P., 2012. Correlations between Stroop task performance and white matter lesion measures in late-onset major depression. Psychiatry Res. 202, 142–149.

de Boer, R., Vrooman, H.A., van der Lijn, F., Vernooij, M.W., Ikram, M.A., van der Lugt, A., Breteler, M.M.B., Niessen, W.J., 2009. White matter lesion extension to automatic brain tissue segmentation on MRI. Neuroimage 45, 1151–1161.

de Groot, M., Ikram, M.A., Akoudad, S., Krestin, G.P., Hofman, A., van der Lugt, A., Niessen, W.J., Vernooij, M.W., 2015. Tract-specific white matter degeneration in aging: The Rotterdam Study. Alzheimer's Dement 11, 321–330.

de Groot, M., Verhaaren, B.F.J., de Boer, R., Klein, S., Hofman, A., van der Lugt, A., Ikram, M.A., Niessen, W.J., Vernooij, M.W., 2013. Changes in normal-appearing white matter precede development of white matter lesions. Stroke 44, 1037–1042.

Debette, S., Markus, H.S., 2010. The clinical importance of white matter hyperintensities on brain magnetic resonance imaging: systematic review and meta-analysis. BMJ 341, c3666.

Farrall, A.J., Wardlaw, J.M., 2009. Blood-brain barrier: ageing and microvascular disease–systematic review and meta-analysis. Neurobiol. Aging 30, 337–352.

Fischl, B., 2012. FreeSurfer. Neuroimage 62, 774–781.

Fridriksson, J., Guo, D., Fillmore, P., Holland, A., Rorden, C., 2013. Damage to the anterior arcuate fasciculus predicts non-fluent speech production in aphasia. Brain 136, 3451–3460.

Friston, K.J., 1998. The disconnection hypothesis. Schizophrenia Res. 30, 115–125.

Gorgolewski, K., Burns, C.D., Madison, C., Clark, D., Halchenko, Y.O., Waskom, M.L., Ghosh, S.S., 2011. Nipype: a flexible, lightweight and extensible neuroimaging data processing framework in Python. Front. Neuroinform 5, 15.

Griebe, M., Amann, M., Hirsch, J.G., Achtnichts, L., Hennerici, M.G., Gass, A., Szabo, K., 2014. Reduced functional reserve in patients with age-related white matter changes: a preliminary fMRI study of working memory. PLoS One 9, e103359.

Griffanti, L., Salimi-Khorshidi, G., Beckmann, C.F., Auerbach, E.J., Douaud, G., Sexton, C.E., Zsoldos, E., Ebmeier, K.P., Filippini, N., Mackay, C.E., Moeller, S., Xu, J., Yacoub, E., Baselli, G., Ugurbil, K., Miller, K.L., Smith, S.M., 2014. ICA-based artefact removal and accelerated fMRI acquisition for improved resting state network imaging. Neuroimage 95, 232–247.

Hofman, A., Brusselle, G.G.O., Darwish Murad, S., van Duijn, C.M., Franco, O.H., Goedegebure, A., Ikram, M.A., Klaver, C.C.W., Nijsten, T.E.C., Peeters, R.P., Stricker, B.H.C., Tiemeier, H.W., Uitterlinden, A.G., Vernooij, M.W., 2015. The Rotterdam Study: 2016 objectives and design update. Eur. J. Epidemiol. 30, 661–708.

Ikram, M.A., van der Lugt, A., Niessen, W.J., Koudstaal, P.J., Krestin, G.P., Hofman, A., Bos, D., Vernooij, M.W., 2015. The Rotterdam Scan Study: design update 2016 and main findings. Eur. J. Epidemiol. 30, 1299–1315.

Jenkinson, M., Bannister, P., Brady, M., Smith, S., 2002. Improved optimization for the robust and accurate linear registration and motion correction of brain images. Neuroimage 17, 825–841.

Jenkinson, M., Beckmann, C.F., Behrens, T.E.J., Woolrich, M.W., Smith, S.M., 2012. Fsl. Neuroimage 62, 782–790.

Johnston, J.M., Vaishnavi, S.N., Smyth, M.D., Zhang, D., He, B.J., Zempel, J.M., Shimony, J.S., Snyder, A.Z., Raichle, M.E., 2008. Loss of resting interhemispheric functional connectivity after complete section of the corpus callosum. J. Neurosci. 28, 6453–6458.

Maillard, P., Carmichael, O., Harvey, D., Fletcher, E., Reed, B., Mungas, D., DeCarli, C., 2013. FLAIR and diffusion MRI signals are independent predictors of white matter hyperintensities. AJNR. Am. J. Neuroradiol 34, 54–61.

O'Reilly, J.X., Croxson, P.L., Jbabdi, S., Sallet, J., Noonan, M.P., Mars, R.B., Browning, P.G.F., Wilson, C.R.E., Mitchell, A.S., Miller, K.L., Rushworth, M.F.S., Baxter, M.G., 2013. Causal effect of disconnection lesions on interhemispheric functional connectivity in rhesus monkeys. Proc. Natl. Acad. Sci. U. S. A. 110, 13982–13987.

Pantoni, L., 2010. Cerebral small vessel disease: from pathogenesis and clinical characteristics to therapeutic challenges. Lancet Neurol. 9, 689–701.

Risse, G.L., LeDoux, J., Springer, S.P., Wilson, D.H., Gazzaniga, M.S., 1978. The anterior commissure in man: functional variation in a multisensory system. Neuropsychologia 16, 23–31.

Salimi-Khorshidi, G., Douaud, G., Beckmann, C.F., Glasser, M.F., Griffanti, L., Smith, S.M., 2014. Automatic denoising of functional MRI data: combining independent component analysis and hierarchical fusion of classifiers. Neuroimage 90, 449–468.

Schonberg, T., Pianka, P., Hendler, T., Pasternak, O., Assaf, Y., 2006. Characterization of displaced white matter by brain tumors using combined DTI and fMRI. Neuroimage 30, 1100–1111.

Seghier, M.L., Lazeyras, F., Zimine, S., Maier, S.E., Hanquinet, S., Delavelle, J., Volpe, J.J., Huppi, P.S., 2004. Combination of event-related fMRI and diffusion tensor imaging in an infant with perinatal stroke. Neuroimage 21, 463–472.

Song, J., Young, B.M., Nigogosyan, Z., Walton, L.M., Nair, V a, Grogan, S.W., Tyler, M.E., Farrar-Edwards, D., Caldera, K.E., Sattin, J.A., Williams, J.C., Prabhakaran, V., 2014. Characterizing relationships of DTI, fMRI, and motor recovery in stroke rehabilitation utilizing brain-computer interface technology. Front. Neuroeng 7, 31.

Starr, J.M., Leaper, S.A., Murray, A.D., Lemmon, H.A., Staff, R.T., Deary, I.J., Whalley, L.J., 2003. Brain white matter lesions detected by magnetic resonance imaging are associated with balance and gait speed. J. Neurol. Neurosurg. Psychiatry 74, 94–98.

Tyszka, J.M., Kennedy, D.P., Adolphs, R., Paul, L.K., 2011. Intact bilateral resting-state networks in the absence of the corpus callosum. J. Neurosci. 31, 15154–15162.

Uddin, L.Q., Mooshagian, E., Zaidel, E., Scheres, A., Margulies, D.S., Kelly, A.M.C., Shehzad, Z., Adelstein, J.S., Castellanos, F.X., Biswal, B.B., Milham, M.P., 2008. Residual functional connectivity in the split-brain revealed with resting-state functional MRI. Neuroreport 19, 703–709.

van Meer, M.P.A., van der Marel, K., Wang, K., Otte, W.M., El Bouazati, S., Roeling, T.A.P., Viergever, M.A., Berkelbach van der Sprenkel, J.W., Dijkhuizen, R.M., 2010. Recovery of sensorimotor function after experimental stroke correlates with restoration of resting-state interhemispheric functional connectivity. J. Neurosci. 30, 3964–3972.

Verhaaren, B.F.J., Vernooij, M.W., de Boer, R., Hofman, A., Niessen, W.J., van der Lugt, A., Ikram, M.A., 2013. High blood pressure and cerebral white matter lesion progression in the general population. Hypertension 61, 1354–1359.

Vernooij, M.W., Ikram, M.A., Vrooman, H.A., Wielopolski, P.A., Krestin, G.P., Hofman, A., Niessen, W.J., Van der Lugt, A., Breteler, M.M.B., 2009. White matter microstructural integrity and cognitive function in a general elderly population. Arch. Gen. Psychiatry 66, 545–553.

Vrooman, H.A., Cocosco, C.A., van der Lijn, F., Stokking, R., Ikram, M.A., Vernooij, M.W., Breteler, M.M.B., Niessen, W.J., 2007. Multi-spectral brain tissue segmentation using automatically trained k-nearest-neighbor classification. Neuroimage 37, 71–81.

Wakana, S., Jiang, H., Nagae-Poetscher, L.M., van Zijl, P.C.M., Mori, S., 2004. Fiber tract-based atlas of human white matter anatomy. Radiology 230, 77–87.

Zhou, Y., Yu, F., Duong, T.Q., 2015. White matter lesion load is associated with resting state functional MRI activity and amyloid PET but not FDG in mild cognitive impairment and early Alzheimer's disease patients. J. Magn. Reson. Imaging 41, 102–109.